

Article

Utilization of the MgO-Rich Residue Originated from Ludwigite Ore: Hydrothermal Synthesis of MHSW Whiskers

Guanghui Li , Li Fang, Xin Zhang, Binjun Liang, Mingjun Rao * , Zhiwei Peng * and Tao Jiang

School of Minerals Processing and Bioengineering, Central South University, Changsha 410083, China; liguangh@csu.edu.cn (G.L.); fanglicsu@126.com (L.F.); csukab@126.com (X.Z.); liangbinjun1205@163.com (B.L.); jiangtao@csu.edu.cn (T.J.)

* Correspondence: raomingjun2003@126.com (M.R.); zwpeng@csu.edu.cn (Z.P.);

Tel.: +86-731-8883-0542 (M.R. & Z.P.)

Received: 14 June 2017; Accepted: 30 July 2017; Published: 4 August 2017

Abstract: In this work, from the MgO-enriched residue originated from ludwigite ore, value-added magnesium hydroxide sulfate hydrate (MHSW) whiskers were prepared via sulfuric acid leaching and leachate purification, followed by hydrothermal synthesis. During sulfuric acid leaching, 98.2% magnesium and 99.6% silica were removed under the optimal leaching conditions: sulfuric acid concentration of 40%, leaching temperature of 80 °C, leaching time of 90 min, and liquid to solid ratio of 4 mL/g. After purification of the acidic leachate via oxidation and precipitation to remove impurities including iron and aluminum, the Mg²⁺-rich solution was used to prepare magnesium hydroxide sulfate hydrate whiskers (5Mg(OH)₂·MgSO₄·2H₂O, abbreviated as 512MHSW) via hydrothermal synthesis. Finally, 512MHSW whiskers were obtained with 30–100 μm in length, 0.5–1.0 μm in diameter and aspect ratio of approximately 100. The physicochemical characteristics of whiskers were further characterized by X-Ray Diffraction (XRD), Scanning Electron Microscopy-Energy Dispersive Spectroscopy (SEM-EDS), Fourier Transform Infrared Spectroscopy (FT-IR) and Thermogravimetry-Differential Scanning Calorimetry (TG-DSC).

Keywords: magnesium hydroxide sulfate hydrate whiskers; hydrothermal synthesis; ludwigite ore; magnesium

1. Introduction

Magnesium hydroxide sulfate hydrate (MHSW) is a group of magnesium salts with a general formula of $x\text{Mg}(\text{OH})_2 \cdot y\text{MgSO}_4 \cdot z\text{H}_2\text{O}$ (referred to as xyz MHSW, including type 513, 512, 123, 318, 131, etc.) [1,2]. MHSW whiskers are important inorganic materials [3,4], with various distinctive properties including low toxicity, high corrosion resistance, low density, high thermal stability and high elastic modulus [5–9], which have been widely used as resin additives of flame retardant for polymers, fillers, reinforcing agent, and acidic waste neutralizer for environmental protection, etc. [10–13]. MHSW whiskers are usually prepared via hydrothermal synthesis [1,14,15]. By using MgSO₄ and NH₃·H₂O as the starting materials, MHSW whiskers with an aspect ratio larger than 100 were synthesized at 150 °C for 16 h [5]. Moreover, a variety of magnesium sources such as magnesium hydroxide, magnesium oxide, magnesium sulfate [16,17], as well as raw serpentine and magnesite ores or even serpentine mine tailings [18], were also used as the starting materials.

Ludwigite ore is rich in boron, iron and magnesium. Its comprehensive utilization has been attempted by using various technologies [19–21], with an emphasis on the recovery of boron and iron rather than magnesium [22,23]. Therefore, it's more beneficial to make use of magnesium component for the

production of value-added products, in addition to the recovery of boron and iron [24]. In our previous studies, a process for stepwise recovery of metallic iron and borate from a ludwigite ore based on coal-based direct reduction has shown its potential and promising future [25,26]. After reductive roasting in the presence of soda ash, 72.1% boron and 95.7% iron were extracted in the forms of sodium metaborate and powdery metallic iron, respectively. As boron and iron could be recovered efficiently, magnesium could also be enriched in the nonmagnetic material to a great extent (about 40 wt % MgO). Due to the transformation of magnesium-containing minerals during soda-ash roasting, the non-magnetic material has excellent solubility in acidic liquor. Therefore, the no-magnetic material with high MgO content could be used as a potential magnesium source for the synthesis of MHSW whiskers.

In this study, MgO-enriched residue derived from ludwigite ore was used as the starting material to prepare MHSW whiskers via acid leaching, leachate purification and hydrothermal synthesis. Acid-leaching characteristics of the MgO-enriched residue were evaluated. After removing the impurities of acid leachate, hydrothermal synthesis was then performed to prepare MHSW whiskers.

2. Experimental

2.1. Materials

2.1.1. MgO-Enriched Residue

The MgO-enriched residue was obtained from ludwigite ore after coal-based reduction roasting, ball mill grinding-water leaching, and magnetic separation [27]. The production process is schematically described in Figure 1.

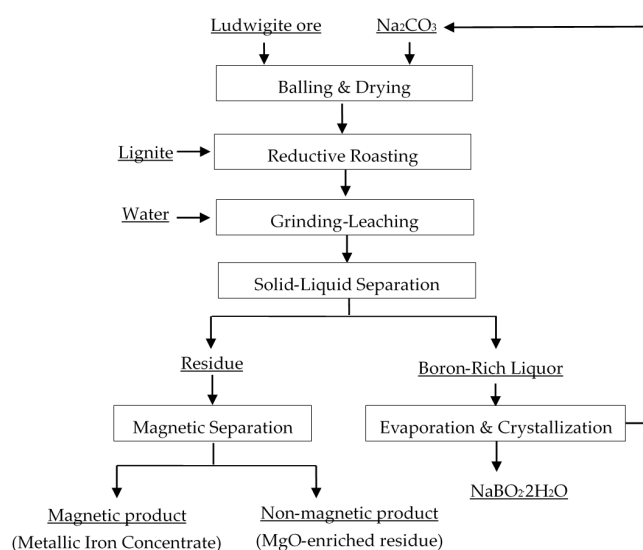


Figure 1. Process for extracting iron and boron from ludwigite ore [27].

The chemical composition of the MgO-enriched residue is shown in Table 1, which was characterized by high magnesium (43.54 wt % MgO) and silicon (16.07 wt % SiO₂) contents. The X-ray diffraction (XRD) pattern in Figure 2 indicates that the major MgO-enriched residue components were magnesium oxide (MgO), magnesium ferrous oxide (Mg_{0.91}Fe_{0.09}O) and disodium magnesium silicate (Na₂MgSiO₄).

Table 1. Main chemical composition of MgO-enriched non-magnetic material (wt %).

MgO	SiO ₂	Na ₂ O	Fe	B ₂ O ₃	Al ₂ O ₃	CaO	¹ LOI
43.54	16.07	12.03	5.91	1.58	0.98	2.52	15.18

¹ LOI is the mass loss on ignition.

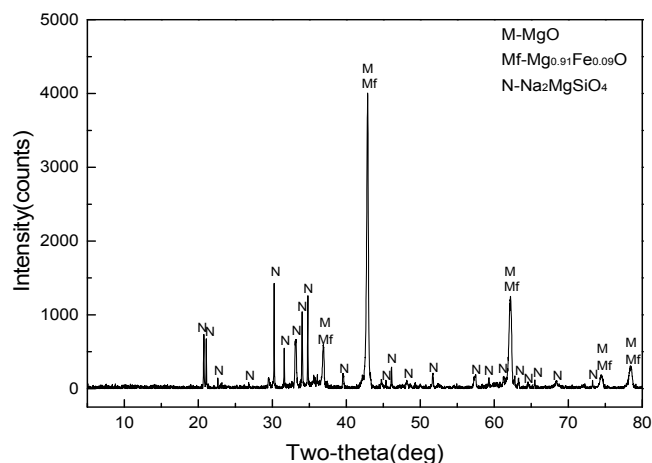


Figure 2. XRD pattern of the MgO-enriched residue.

2.1.2. Chemical Regents

Sulfuric acid, hydrogen peroxide, magnesia and sodium hydroxide were used in the experiments. All of these chemicals were of analytical reagent grade.

2.2. Methods

2.2.1. Experimental Procedure

The flow sheet for preparing MHSW whiskers is shown in Figure 3, including: (1) Leaching MgO-enriched residue with sulfuric acid to obtain leachate containing magnesium sulfate after separation of silica; (2) Removing impurities of acidic leachate by oxidation and precipitation; and (3) Preparing MHSW whiskers via hydrothermal synthesis.

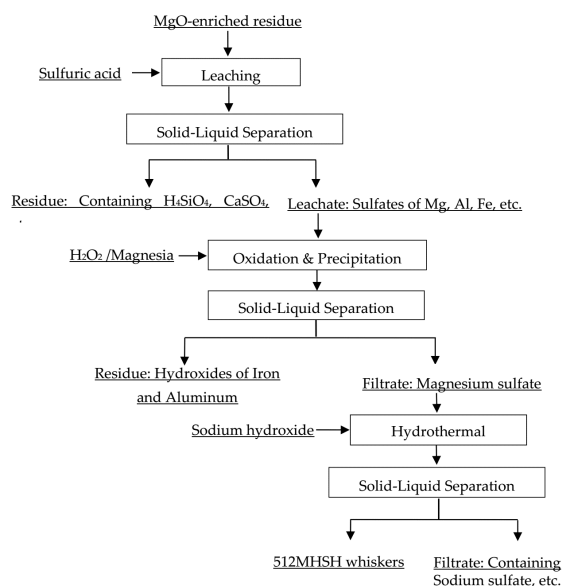


Figure 3. Experimental flow sheet for preparing magnesium hydroxide sulfate hydrate (MHSW) whiskers by using MgO-enriched residue.

2.2.2. Sulfuric Acid Leaching of MgO-Enriched Residue

Leaching experiments were carried out in a 250-mL beaker immersed in a temperature-controlled electrically heated water bath installed with a plastic stirrer. At the beginning of each test, the MgO-enriched

residue was added into the beaker and mixed with sulfuric acid solution with the liquid-to-solid ratio ranging from 3 to 7 mL/g. Then, the beaker was soaked in the bath at a given temperature and agitated for a specified period of time. After filtration, the residue was washed with hot water and dried at 105 °C in a drying oven. The leaching ratio of constituents (μ) was calculated as follows:

$$\mu = \frac{C_t \cdot V_t}{m_t \cdot \alpha_t} \times 100\% \quad (1)$$

where μ is the leaching ratio, %; C_t is the constituents content of leaching solution; V_t is the volume of leaching solution, mL; α_t is the constituents content of MgO-enriched residue; and m_t is the mass of MgO-enriched residue.

2.2.3. Purification of Acidic Leachate

Sulfuric acid leachate was charged into a beaker before adding a few drops of potassium ferricyanide as a reaction indicator. Then, hydrogen peroxide was slowly added to oxidize Fe^{2+} to Fe^{3+} until the solution's color changed from light green to yellow. The magniferous solution was added to adjust the pH value to 5.7. The whole process was conducted at a certain temperature and stirring speed. The residue (hydroxides of Fe and Al) was separated from leaching solution and washed with hot water. The removal ratio of impurities (θ) and retention ratio of magnesium (γ) were calculated as follows:

$$\theta = \frac{m_p \cdot \alpha_p}{C_t \cdot V_0} \times 100\% \quad (2)$$

$$\gamma = \left(1 - \frac{m_p \cdot \alpha_q}{C_t \cdot V_0}\right) \times 100\% \quad (3)$$

where α_p and α_q are the content of impurities and magnesium of the precipitate respectively; m_p is the weight of the precipitate; C_t and V_0 are the constituents content and volume of leachate used in the impurities removal experiments, respectively.

2.2.4. Hydrothermal Synthesis

Hydrothermal synthesis was conducted in an electrically heated autoclave equipped with a one-liter stainless steel tank and plastic stirrer. The synthesis temperature was controlled by a thermostat. For preparing 512MHSW whiskers, the purified $MgSO_4$ solution was added with NaOH (1 mol/L) with various mole ratio in the autoclave. The autoclave was then heated to 120–200 °C and kept under isothermal condition for 0.5–7 h. A white slurry was obtained after the autoclave was cooled down to the room temperature naturally. After filtration, the precipitate was washed with distilled water and then dried in a vacuum oven at 100 °C for 10 h to obtain the whiskers.

2.2.5. Instrumental Analyses

The chemical compositions of the samples were examined using an X-ray fluorescence spectrometer (XRF, PANalytical, Axios mAX, Almelo, The Netherlands). The mineral constituents were determined by X-ray diffraction spectrometer (XRD, Rigaku, D/Max 2500, Tokyo, Japan), using a Cu-anode target with the wavelength of 1.54056 Å, scan mode for the step scan, step length of 0.02°. The morphologies of MHSW whiskers were characterized by using scanning electron microscopy (SEM, JEOL, JSM-6360LM, Tokyo, Japan) equipped with an energy dispersive spectrometer (EDS). The infrared spectrum of MHSW whiskers was characterized by using Fourier transform infrared spectroscopy (FT-IR, 830, Shimadzu, Kyoto, Japan). The thermal decomposition behavior of MHSW whiskers were characterized using thermogravimetric analysis (TG-DSC, NETZSCH, STA449C, Selb, Germany). The temperature range covered was 30–1400 °C, with a heating rate of 10 °C/min and argon gas flow of 20 mL/min.

3. Results and Discussion

3.1. Separation and Purification of Magnesium Sulfate from MgO-Enriched Residue

3.1.1. Sulfuric-Acid Leaching Behavior of Magnesium from MgO-Enriched Residue

Effects of leaching temperature, leaching time, sulfuric acid concentration and liquid-to-solid (L/S) ratio on the magnesium dissolution of MgO-enriched residue were examined at a fixed stirring speed of 300 r/min, and the corresponding results are shown in Figure 4.

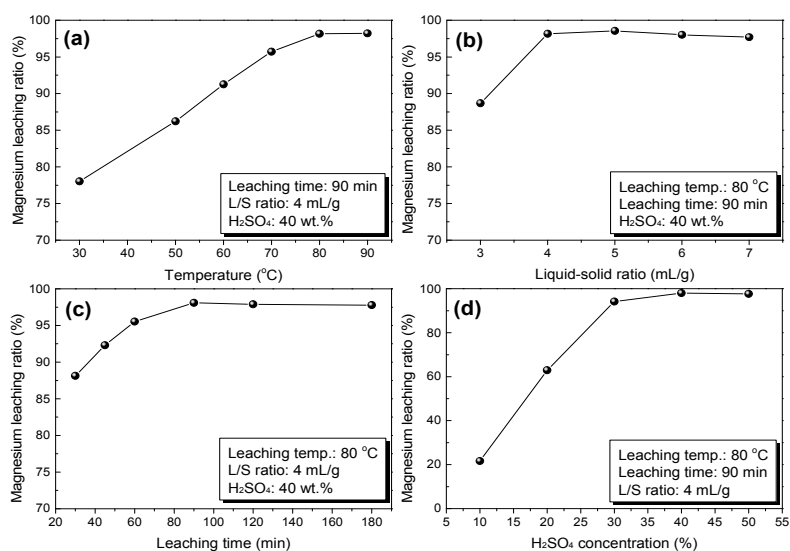


Figure 4. Extraction of magnesium as the function of (a) leaching temperature; (b) liquid-to-solid ratio; (c) leaching time; and (d) sulfuric acid concentration.

The leaching ratio of magnesium increased with leaching temperature, time, sulfuric acid concentration and L/S ratio (Figure 4). However, for each variable, the leaching ratio leveled off after a certain value. For temperature, liquid solid ratio, leaching time and acid concentration, these values were determined to be 80 °C, 4, 90 min and 40% sulfuric acid respectively.

From the above results, the optimal parameters for the conversion of magnesium oxide into magnesium sulfate were obtained. The leaching ratio of magnesium reached about 98% under the following leaching conditions: sulfuric acid concentration of 30–40 wt %, leaching temperature of 70–90 °C, leaching time of 90 min, and L/S ratio of 4 mL/g.

By comparing Figures 2 and 5, it was found that magniferous minerals were dissolved by sulfuric acid, leaving amorphous silica gel and calcium sulfate in the leaching residue. Table 2 shows that the leaching residue contains 67.7 wt % SiO₂ and 13.98 wt % CaSO₄, which could be further used to prepare white carbon black or lithium silicate material.

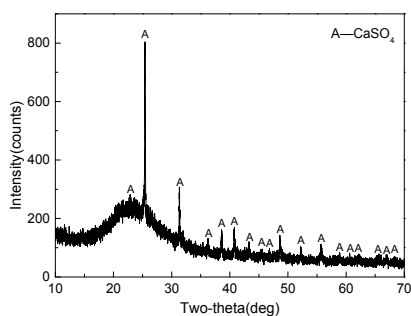
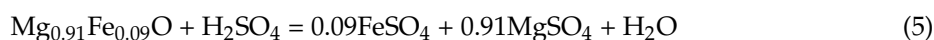


Figure 5. X-ray diffraction (XRD) pattern of acid leaching residue.

Table 2. Main chemical composition of acid leaching residue (wt %).

Compositions	SiO ₂	MgO	Fe ₂ O ₃	Al ₂ O ₃	CaSO ₄	Na ₂ O	B ₂ O ₃	LOI
content/%	67.76	1.63	2.54	0.28	13.98	0.42	0.07	12.21

By comparing the composition of the MgO-enriched residue with that of sulfuric acid-leaching residue, it can be deduced that magnesia and silica were well dissolved. The corresponding reactions are represented as:



3.1.2. Precipitating Impurities of Acidic Leachate

Under the optimal conditions of sulfuric acid leaching of MgO-enriched residue, the leaching of different constituents is shown in Table 3.

Table 3. Result of sulfuric acid leaching of MgO-enriched residue.

Composition	Si	Mg	Fe	Al	Ca	Na	B
Acid leaching solution (g/L)	0.054	51.29	11.29	0.96	1.65	17.59	0.92
Leaching ratio (%)	0.4	98.2	95.5	93.2	45.8	98.5	98.9

As can be seen from Table 3, impurity ions such as Fe³⁺, Fe²⁺ and Al³⁺ existed in the leachate. The presence of these impurity ions will deteriorate the quality of the MSH whiskers during hydrothermal synthesizing. Therefore, it is necessary to remove Fe³⁺, Fe²⁺ and Al³⁺ in advance.

Table 4 shows that the pH value range for the precipitation of Mg²⁺ is different from those of Fe³⁺, Fe²⁺, Al³⁺, but the complete precipitation pH of Fe²⁺ is close to the starting precipitation pH of Mg²⁺. By adding hydrogen peroxide to oxidize Fe²⁺ to Fe³⁺, the differences of precipitating pH values between Mg²⁺ and impurity ions could be enlarged. In this way, Fe³⁺, Fe²⁺ and Al³⁺ ions are removed according to the following reactions [28]:

**Table 4.** Metal hydroxides precipitation pH value and solubility product constant Ksp value.

Ions	Fe ³⁺	Fe ²⁺	Al ³⁺	Mg ²⁺
Starting precipitation pH	1.6	6.5	3.3	9.4
Complete precipitation pH	3.2	9.7	5.2	12.4
Ksp	4.0 × 10 ⁻³⁸	8.0 × 10 ⁻¹⁶	1.9 × 10 ⁻³⁶	9.6 × 10 ⁻³

Under the conditions of pH of 5.7, reaction time of 30 min and reaction temperature of 60 °C, the retention ratio of magnesium was 98.1%, while the Fe³⁺ and Al³⁺ removal ratios reached 99.6% and 99.9%, respectively. The elemental concentration of the purified solution after oxidation and precipitation is shown in Table 5. Obviously, the purified solution is more suitable for the downstream preparation of value-added products.

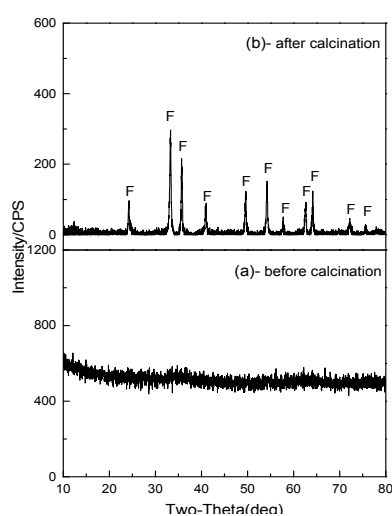
Table 5. Elemental concentration of purified solution (g/L).

Mg	Na	Fe	Al	Si	B
64.40	7.27	2.75×10^{-3}	0.05×10^{-3}	0.17×10^{-3}	0.686

The chemical composition of precipitate is shown in Table 6, showing that the precipitate mainly constitutes of Fe_2O_3 (60.63 wt %). XRD patterns of the precipitate before and after calcination (at 600 °C for 60 min) are shown in Figure 6.

Table 6. Chemical composition of precipitate without calcination (wt %).

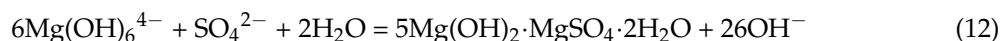
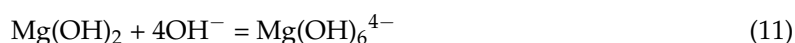
Al_2O_3	SiO_2	Fe_2O_3	CaO	MgO	Na_2O	S
4.30	0.7	60.63	0.13	1.27	0	2.02

**Figure 6.** XRD patterns of the precipitate (a) before and (b) after calcination (F- Fe_2O_3).

3.2. Preparing MHSW Whiskers from Acidic Leachate

During hydrothermal synthesis, Mg^{2+} in the solution initially reacted with OH^- from NaOH to form $\text{Mg}(\text{OH})_2$ (Equation (10)). At high temperatures, the $\text{Mg}(\text{OH})_2$ precursor dissolved and underwent hydrolysis to produce $\text{Mg}(\text{OH})_6^{4-}$ (Equation (11)). Then the reaction of $\text{Mg}(\text{OH})_6^{4-}$ with SO_4^{2-} of the solution resulted in MHSW (Equation (12)). Due to the low solubility of $\text{Mg}(\text{OH})_2$, an excess amount of MgSO_4 was necessary for the growth of whiskers.

The corresponding formation of 512MHSW whiskers can be expressed as:



3.2.1. Effect of MgSO_4 Concentration

The effect of MgSO_4 concentration on the morphology and phase composition of the obtained whiskers was evaluated under the conditions of $n(\text{MgSO}_4):n(\text{NaOH}) = 2:1$, NaOH concentration of 1 mol/L, hydrothermal processing at 180 °C for 4 h, and stirring speed of 300 r/min.

As shown in Figures 7 and 8, when the MgSO_4 concentration was 1.5 mol/L, the synthesized product was $\text{Mg}(\text{OH})_2$ and no whiskers were formed. However, when the MgSO_4 concentration reached 2.5 mol/L, the morphology of 512MHSW whiskers became more regular, and the maximum

aspect ratio exceeded 100. The lengths of whiskers changed slightly with the increasing concentration of MgSO_4 to 3.0 mol/L. Overall, the MgSO_4 concentration of 2.5–3.0 mol/L was suitable for the hydrothermal synthesis of 512MHSW whiskers.

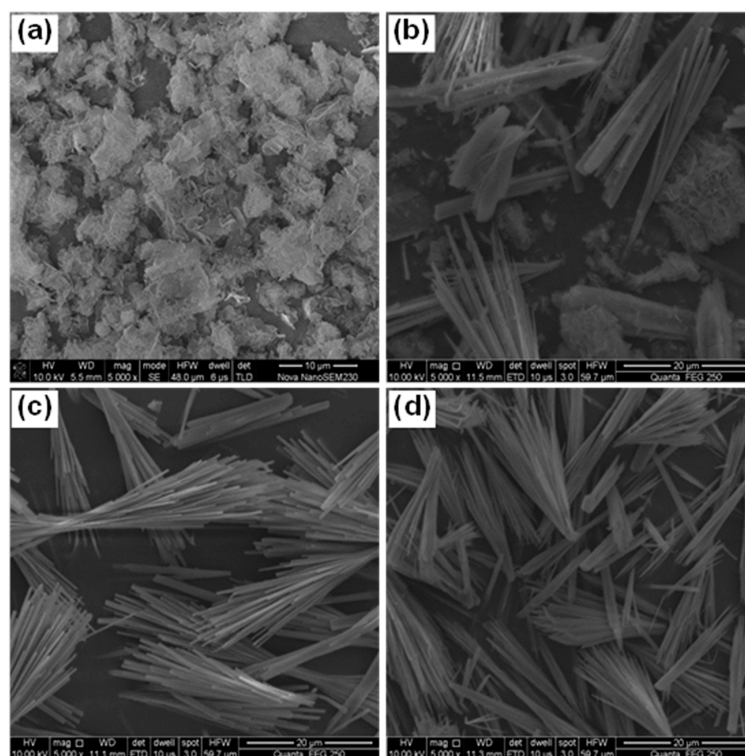


Figure 7. Scanning electron microscopy (SEM) images of whiskers obtained at different MgSO_4 concentrations (a) 1.5 mol/L; (b) 2.25 mol/L; (c) 2.5 mol/L; (d) 3.0 mol/L.

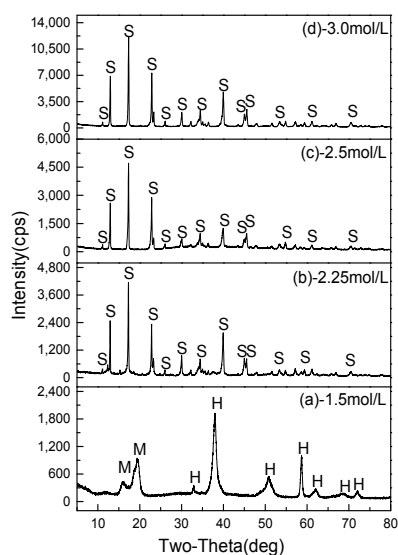


Figure 8. XRD patterns of whiskers obtained at different MgSO_4 concentrations H- $\text{Mg}(\text{OH})_2$, S- $5\text{Mg}(\text{OH})_2 \cdot \text{MgSO}_4 \cdot 2\text{H}_2\text{O}$, M- $\text{MgSO}_4 \cdot x\text{H}_2\text{O}$.

3.2.2. Effect of Mole Ratio of $\text{MgSO}_4/\text{NaOH}$

The effect of the mole ratio of $\text{MgSO}_4/\text{NaOH}$ on the morphology and structure of the whiskers was studied under the conditions of the MgSO_4 concentration of 2.5 mol/L, NaOH concentration of

high-quality 512MHSW whiskers with a maximum aspect ratio of about 100 and smooth surface were obtained. Nevertheless, 512MHSW whiskers gradually converted to $\text{Mg}(\text{OH})_2$ with the further decrease of $\text{MgSO}_4/\text{NaOH}$ mole ratio. Thus, the optimum mole ratio of $\text{MgSO}_4/\text{NaOH}$ was 2.

3.2.3. Effect of Hydrothermal Temperature

Effects of hydrothermal temperature on the morphology and phase composition of whiskers were studied under the conditions of $n(\text{MgSO}_4):n(\text{NaOH}) = 2:1$, MgSO_4 concentration of 2.5 mol/L, NaOH concentration of 1 mol/L, hydrothermal duration of 4 h, and stirring speed of 300 r/min.

From Figures 11 and 12, there were no 512MHSW whiskers at 120 °C. The morphology of whiskers became regular with increasing temperature. 512MHSW whiskers with high aspect ratio of 100 and smooth surface in the absence of $\text{Mg}(\text{OH})_2$ impurities were successfully synthesized at 180 °C, but the 512MHSW whiskers disappeared when the temperature was further increased to 200 °C. Thus, the optimal hydrothermal temperature range was 160–180 °C.

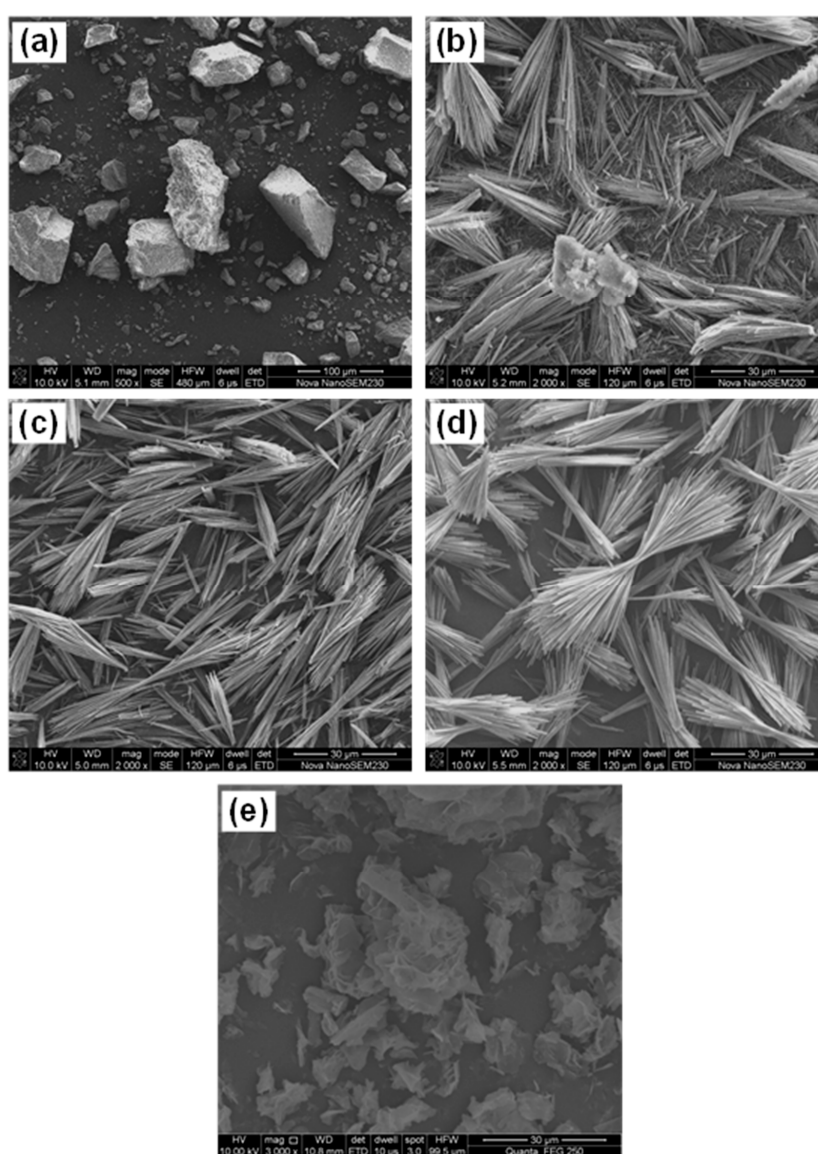


Figure 11. SEM images of whiskers obtained at different hydrothermal temperatures (a) 120 °C; (b) 140 °C; (c) 160 °C; (d) 180 °C; (e) 200 °C.

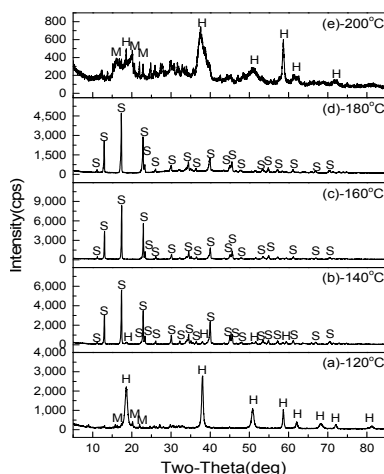


Figure 12. XRD patterns of whiskers obtained at different hydrothermal temperatures H-Mg(OH)_2 , $\text{S-5Mg(OH)}_2 \cdot \text{MgSO}_4 \cdot 2\text{H}_2\text{O}$, $\text{M-MgSO}_4 \cdot x\text{H}_2\text{O}$.

3.2.4. Effect of Hydrothermal Duration

Effects of hydrothermal duration on the morphology and phase of whiskers were studied under the conditions of $n(\text{MgSO}_4):n(\text{NaOH}) = 2:1$, MgSO_4 concentration of 2.5 mol/L, NaOH concentration of 1 mol/L, hydrothermal temperature of 180 °C, and stirring speed of 300 r/min.

Figures 13 and 14 show morphologies of whiskers synthesized by varying the hydrothermal duration from 0.5 to 7 h. The morphologies became more complete with the extension of hydrothermal time. The 512MHSW whiskers only presented a few sporadic whiskers with short fiber length in 0.5 h. When the hydrothermal duration was extended to 4 h, the whiskers gradually grew to be smooth with a uniform aspect ratio of about 100. Whiskers, however, were destroyed once again when the hydrothermal duration further increased to 7 h.

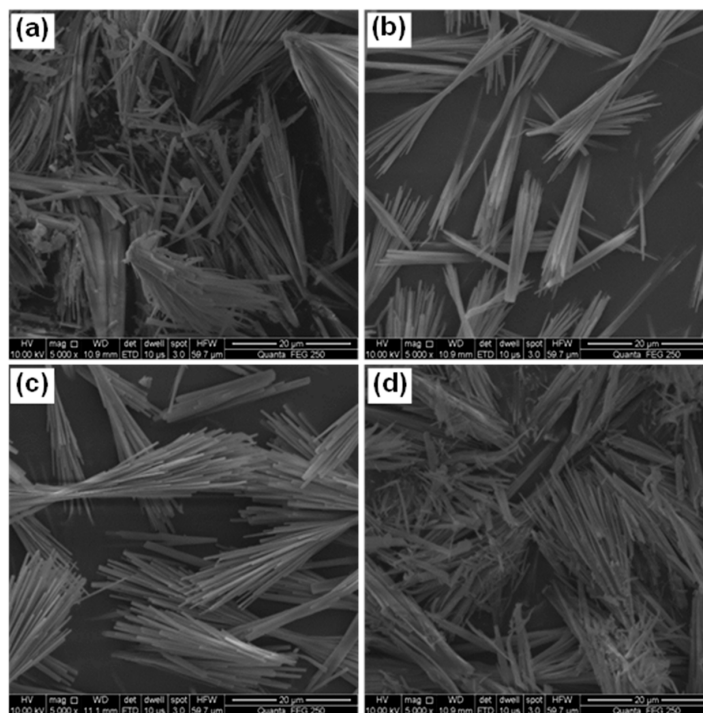


Figure 13. Morphologies of whiskers obtained at different hydrothermal durations (a) 0.5 h; (b) 2 h; (c) 4 h; (d) 7 h.

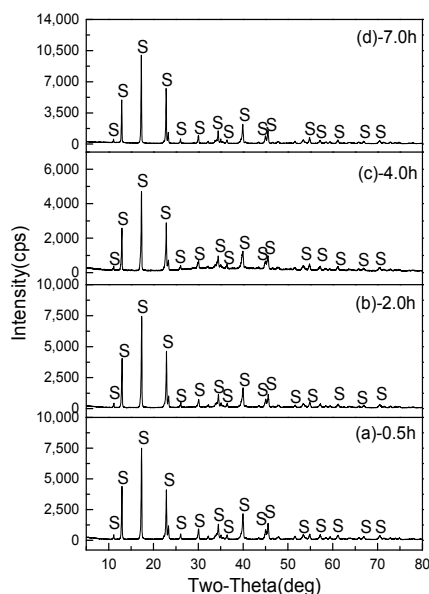


Figure 14. XRD patterns of whiskers obtained at different hydrothermal periods of time $S\text{-}5\text{Mg}(\text{OH})_2\cdot\text{MgSO}_4\cdot 2\text{H}_2\text{O}$.

Based on the above results, the optimal hydrothermal synthesis conditions for preparing 512MHSW whiskers are as follows: 2.5–3.0 mol/L MgSO_4 in 1.0 mol/L NaOH solution for a fixed $\text{MgSO}_4/\text{NaOH}$ mole ratio of 2 at 160–180 °C for 2.0–4.0 h. Under these conditions, the 512MHSW whiskers with a length of 30–100 μm , an average diameter of 0.5–1.0 μm and an aspect ratio of ~ 100 were produced.

3.3. Characterization of MHSW Whiskers

3.3.1. XRD

The XRD pattern of the hydrothermal product, prepared under the optimal hydrothermal synthesis conditions, is shown in Figure 15. All the diffraction peaks can be indexed to the orthorhombic structure of $5\text{Mg}(\text{OH})_2\cdot\text{MgSO}_4\cdot 2\text{H}_2\text{O}$ (PDF No. 86-1322).

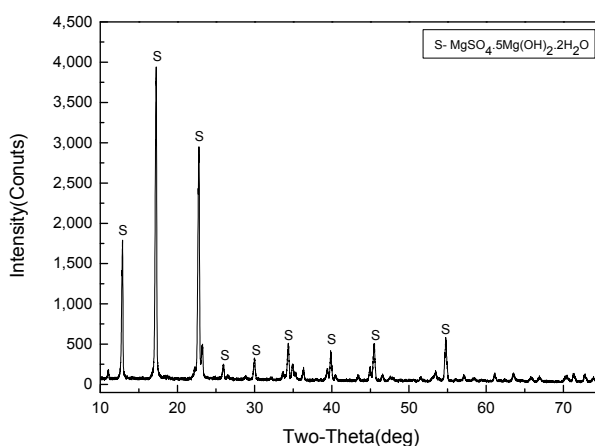


Figure 15. XRD pattern of the hydrothermal product.

3.3.2. SEM-EDS

It can be observed that the hydrothermal product has needle-like morphology with sector-like ends (Figure 16). The whiskers have a length of 30–100 μm and an average diameter of 0.5–1.0 μm .

The EDS spectrum indicates that the ratio of Mg to S is very close to the stoichiometric value of $5\text{Mg}(\text{OH})_2 \cdot \text{MgSO}_4 \cdot 2\text{H}_2\text{O}$.

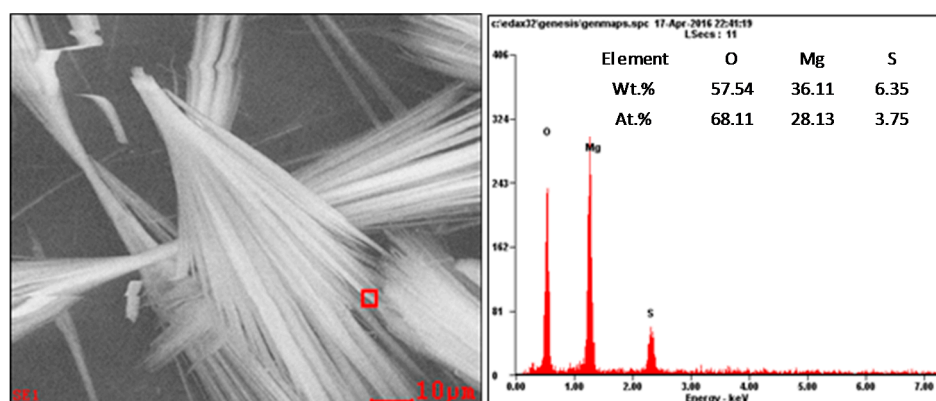


Figure 16. EDS spectra of the hydrothermal product.

3.3.3. FT-IR

The infrared spectrum of the hydrothermal product is shown in Figure 17. The peaks at 3648.78 and 3611.43 cm^{-1} are assigned to the $-\text{OH}$ stretching vibration. The peak at 3416.40 cm^{-1} is the hydrogen bond formed by reactions of hydroxyls. The peak at 1628.19 cm^{-1} is due to the bending vibration of the $-\text{OH}$ bond. The peak at 815.91 cm^{-1} is the coordination bond between H_2O and Mg^{2+} . Two sharp absorption bands at 1116.89 and 639.52 cm^{-1} are ascribed to the $\text{O}-\text{S}-\text{O}$ bond.

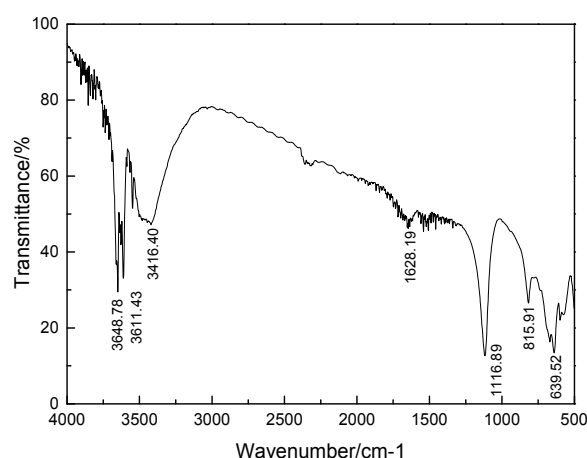


Figure 17. Fourier transform infrared spectroscopy FT-IR pattern of the hydrothermal product.

3.3.4. TG-DSC

TG-DSC curves (Figure 18) of the hydrothermal product exhibit three stages of pronounced weight loss and endothermic effect, respectively. Table 7 compares the weight losses of the hydrothermal product and theoretical values. The first stage of weight loss (7.9%) in the temperature range of $306\text{--}377 \text{ }^\circ\text{C}$ corresponds to the loss of crystal water (Equation (13)). The second stage of weight loss (20.0%) in the temperature range of $386\text{--}641 \text{ }^\circ\text{C}$ corresponds to the loss of hydroxyl water (Equation (14)). The last stage of weight loss (17.8%) in the temperature range of $897\text{--}1029 \text{ }^\circ\text{C}$ corresponds to the desulfation of $\text{MgSO}_4 \cdot 5\text{MgO}$ (Equation (15)).

The thermal decomposition reactions of the hydrothermal product can be expressed as:



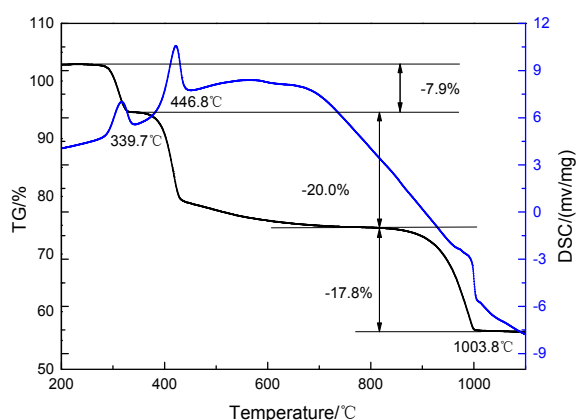
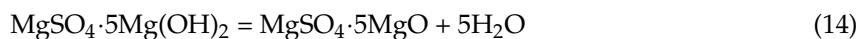


Figure 18. Thermogravimetry-differential scanning calorimetry TG-DSC curves of the hydrothermal product.

Table 7. The comparison of mass loss of the product and theoretical value.

Step	Decomposition Temperature/°C	Theoretical Weight Loss/%	Hydrothermal Product Weight Loss/wt %
1	306–377	8.04	7.9
2	386–641	20.10	20.0
3	897–1029	17.89	17.8

4. Conclusions

High-quality 512MHSW whiskers were prepared from the MgO-enriched residue derived from ludwigite ore by sulfuric acid leaching followed by hydrothermal synthesis. The conclusions can be drawn as follows.

1. During the sulfuric acid leaching of MgO-enriched residue, silica could be effectively separated from magnesium by leaching with 40 wt % sulfuric acid at 80 °C for 90 min with a liquid-solid ratio of 4 mL/g. The leaching ratio of magnesium reached about 98.2% while 99.6% of silica was removed and enriched in the leaching residue. Furthermore, value-added products of silica gel with 67.7% SiO₂ was prepared from the acid leaching residue.
2. The impurities in acidic leachate could be well removed under the conditions of pH of 5.7, reaction time of 30 min and reaction temperature of 60 °C. The magnesium retention ratio was 98.1%, and the iron removal ratio was 99.6 %. Iron oxide red could be obtained as a byproduct from the precipitate.
3. 512MHSW whiskers with a length of 30–100 μm, an average diameter of 0.5–1.0 μm and an aspect ratio of 100 were obtained by hydrothermal synthesis at 160–180 °C for 2.0–4.0 h using the mixed aqueous solution of 2.5–3.0 mol/L MgSO₄ and 1.0 mol/L NaOH solution with a fixed MgSO₄/NaOH mole ratio of 2. The whiskers were featured by smooth surface and small diameter.

Acknowledgments: The authors wish to express their thanks to the National Natural Science Foundation of China (No. 51234008) for financial support. This work was also financially supported by the Co-Innovation Center for Clean and Efficient Utilization of Strategic Metal Mineral Resources.

Author Contributions: Guanghui Li, Mingjun Rao and Zhiwei Peng conceived and designed the experiments; Li Fang and Binjun Liang performed the experiments and analyzed the data; Xin Zhang contributed analysis tools; Guanghui Li, Li Fang, Mingjun Rao, Zhiwei Peng and Tao Jiang wrote and reviewed the paper.

Conflicts of Interest: The authors declare no conflicts of interest. The founding sponsors had no role in the design of the study; in the collection, analyses, or interpretation of data; in the writing of the manuscript, and in the decision to publish the results.

References

1. Kang, K.H.; Lee, D.K. Synthesis of magnesium oxysulfate whiskers using triethanolamine as a morphology control agent. *J. Ind. Eng. Chem.* **2014**, *20*, 2580–2583. [[CrossRef](#)]
2. Yan, X.X.; Xu, D.L.; Xue, D.F. SO_4^{2-} ions direct the one-dimensional growth of $5\text{Mg}(\text{OH})_2 \cdot \text{MgSO}_4 \cdot 2\text{H}_2\text{O}$. *Acta Mater.* **2007**, *55*, 5747–5757. [[CrossRef](#)]
3. Dang, L.; Nai, X.Y.; Zhu, D.H.; Jing, Y.W.; Liu, X.; Dong, Y.P.; Li, W. Study on the mechanism of surface modification of magnesium oxysulfate whisker. *Appl. Surf. Sci.* **2014**, *317*, 325–331. [[CrossRef](#)]
4. Zhu, D.H.; Nai, X.; Lan, S.; Bian, S.; Liu, X.; Li, W. Surface modification of magnesium hydroxide sulfate hydrate whiskers using a silane coupling agent by dry process. *Appl. Surf. Sci.* **2016**, *390*, 25–30. [[CrossRef](#)]
5. Ding, Y.; Zhang, G.; Zhang, S.; Huang, X.; Yu, W.; Qian, Y. Preparation and characterization of magnesium hydroxide sulfate hydrate whiskers. *Chem. Mater.* **2000**, *12*, 2845–2852. [[CrossRef](#)]
6. Ma, X.L.; Ning, G.Q.; Qi, C.L.; Gao, J.S. One-step synthesis of basic magnesium sulfate whiskers by atmospheric pressure reflux. *Particuology* **2016**, *24*, 191–196. [[CrossRef](#)]
7. Sun, X.T.; Xiang, L. Hydrothermal conversion of magnesium oxysulfate whiskers to magnesium hydroxide nanobelts. *Mater. Chem. Phys.* **2008**, *109*, 381–385.
8. Wang, X.L.; Xue, D.F. Direct observation of the shape evolution of MgO whiskers in a solution system. *Mater. Lett.* **2006**, *60*, 3160–3164. [[CrossRef](#)]
9. Wei, Z.Q.; Qi, H.; Ma, P.H.; Bao, J.Q. A new route to prepare magnesium oxide whisker. *Inorg. Chem. Commun.* **2002**, *5*, 147–149. [[CrossRef](#)]
10. Gao, C.H.; Li, X.G.; Feng, L.J.; Lu, S.Y.; Liu, J.Y. Surface modification and characterization of magnesium hydroxide sulfate hydrate nanowhiskers. *Appl. Surf. Sci.* **2010**, *256*, 3234–3239. [[CrossRef](#)]
11. Xiang, L.; Liu, F.; Li, J.; Jin, Y. Hydrothermal formation and characterization of magnesium oxysulfate whiskers. *Mater. Chem. Phys.* **2004**, *87*, 424–429. [[CrossRef](#)]
12. Zhao, Y.; Liu, B.; Yang, J.J.; Jia, J.P.; You, C.; Chen, M.F. Effects of modifying agents on surface modifications of magnesium oxide whiskers. *Appl. Surf. Sci.* **2016**, *388*, 370–375. [[CrossRef](#)]
13. Zhao, Y.; Liu, B.; You, C.; Chen, M.F. Effects of MgO whiskers on mechanical properties and crystallization behavior of PLLA/MgO composites. *Mater. Des.* **2016**, *89*, 573–581. [[CrossRef](#)]
14. Liu, C.J.; Zhao, Q.; Wang, Y.G.; Shi, P.Y.; Jiang, M.F. Hydrothermal synthesis of calcium sulfate whisker from flue gas desulfurization gypsum. *Chin. J. Chem. Eng.* **2016**, *24*, 1552–1560. [[CrossRef](#)]
15. Zhou, Z.Z.; Deng, Y.L. Solution synthesis of magnesium hydroxide sulfate hydrate nanobelts using sparingly soluble carbonate salts as supersaturation control agents. *J. Colloid Interface Sci.* **2007**, *316*, 183–188. [[CrossRef](#)] [[PubMed](#)]
16. Ding, Y.; Zhao, H.; Sun, Y.; Zhang, G.; Wu, H.; Qian, Y. Superstructured magnesium hydroxide sulfate hydrate fibres—Photoluminescence study. *Int. J. Inorg. Mater.* **2001**, *3*, 151–156. [[CrossRef](#)]
17. Gao, C.H.; Li, X.G.; Feng, L.J.; Xiang, Z.C.; Zhang, D.H. Preparation and thermal decomposition of $5\text{Mg}(\text{OH})_2 \cdot \text{MgSO}_4 \cdot 2\text{H}_2\text{O}$ nanowhiskers. *J. Chem. Eng.* **2009**, *150*, 551–554. [[CrossRef](#)]
18. Su, X.L.; Sun, C.M.; Chen, Y.X.; Zeng, T. Preparation of basic magnesium sulfate whisker by serpentine mine tailings solid wastes. *Bull. Chin. Ceram. Soc.* **2014**, *33*, 92–96. (In Chinese)
19. An, J.; Xue, X.X. Life cycle environmental impact assessment of borax and boric acid production in China. *J. Clean. Prod.* **2014**, *66*, 121–127. [[CrossRef](#)]
20. Ning, Z.Q.; Zhai, Y.C.; Song, Q.S. Extracting B_2O_3 from calcined boron mud using molten sodium hydroxide. *Rare Met.* **2015**, *34*, 744–751. [[CrossRef](#)]
21. Wang, G.; Xue, Q.G.; Wang, J.S. Effect of Na_2CO_3 on reduction and melting separation of ludwigite/coal composite pellet and property of boron-rich slag. *Trans. Nonferrous Met. Soc. China* **2016**, *26*, 282–293. [[CrossRef](#)]
22. Fu, X.J.; Zhao, J.Q.; Chen, S.Y.; Liu, Z.G.; Guo, T.L.; Chu, M.S. Comprehensive Utilization of Ludwigite Ore Based on Metallizing Reduction and Magnetic Separation. *J. Iron Steel Res. Int.* **2015**, *22*, 672–680. [[CrossRef](#)]

23. Li, Y.L.; Qu, J.K.; Wei, G.Y.; Qi, T. Influence of Na₂CO₃ as Additive on Direct Reduction of Boron-bearing Magnetite Concentrate. *J. Iron Steel Res. Int.* **2016**, *23*, 103–108. [[CrossRef](#)]
24. Ren, W.; Ye, J.; Wang, X.; Gong, W.; Lin, Y.; Ning, G. Study on preparation of basic magnesium sulfate whiskers from boron slurry. *Inorg. Chem. Ind.* **2010**, *42*, 56–59. (In Chinese)
25. Jie, L.I.; Fan, Z.G.; Liu, Y.L.; Liu, S.L.; Tao, J.; Xi, Z.P. Preparation of boric acid from low-grade ascharite and recovery of magnesium sulfate. *Trans. Nonferrous Met. Soc. China* **2010**, *20*, 1161–1165.
26. Liang, B.; Li, G.; Rao, M.; Peng, Z.; Zhang, Y.; Jiang, T. Water leaching of boron from soda-ash-activated ludwigite ore. *Hydrometallurgy* **2017**, *167*, 101–106. [[CrossRef](#)]
27. Li, G.; Liang, B.; Rao, M.; Zhang, Y.; Jiang, T. An innovative process for extracting boron and simultaneous recovering metallic iron from ludwigite ore. *Miner. Eng.* **2014**, *56*, 57–60. [[CrossRef](#)]
28. Luo, Z.; Yang, J.; Ma, H.W.; Liu, M.T.; Ma, X. Recovery of magnesium and potassium from biotite by sulfuric acid leaching and alkali precipitation with ammonia. *Hydrometallurgy* **2015**, *157*, 188–193. [[CrossRef](#)]



© 2017 by the authors. Licensee MDPI, Basel, Switzerland. This article is an open access article distributed under the terms and conditions of the Creative Commons Attribution (CC BY) license (<http://creativecommons.org/licenses/by/4.0/>).